The Report Committee for Craig Robert Ayres
Certifies that this is the approved version of the following Report:

Developing a Socially-Embedded Point-of-Use Water Treatment Strategy Incorporating Silver Nanoparticles and Microwave Radiation

APPROVED BY
SUPERVISING COMMITTEE:

Navid Saleh, Supervisor

Mary Jo Kirisits

Developing a Socially-Embedded Point-of-Use Water Treatment Strategy Incorporating Silver Nanoparticles and Microwave Radiation

by

Craig Ayres

Report

Presented to the Faculty of the Graduate School of

The University of Texas at Austin

in Partial Fulfillment

of the Requirements

for the Degree of

Master of Science in Engineering

The University of Texas at Austin

May 2018

Abstract

Developing a Socially-Embedded Point-of-Use Water Treatment Technology Incorporating Silver Nanoparticles and Microwave Radiation

Craig Robert Ayres, MSE

The University of Texas at Austin, 2018

Supervisor: Navid Saleh

Providing safe drinking water is a multifaceted problem that goes beyond a treatment device and deserves a holistic approach with respect to sanitation, handling, education, and customs of the target community. Socially-embedded point-of-use treatment strategies based on familiar components are more likely to receive prolonged use from the residents. Microwave ovens are a globally diffused, socially accepted technology that are enticing options for foundations of irradiation-based treatment. Taking advantage of the exceptional qualities of certain materials at the nano-scale allows one to utilize the low-energy radiation of microwave rays. This study focused on silver nanoparticles under the hypothesis that increased temperature from microwave exposure would result in increased ion dissolution and heat shock, thus enhancing antimicrobial potency. Using *Escherichia coli* (K12) as a model microorganism, 1 mL samples containing up to 1 mg/L of suspended silver nanoparticles were irradiated in a microwave

reactor (2,450 MHz; 70 W) for 60 and 90 s. A clear synergistic effect between microwave radiation and silver nanoparticles was observed as microbial inactivation increased with additional microwave exposure and higher concentrations of silver. A maximum of 4.7 $\log_{10}$ reduction was achieved after 90 s of irradiation, indicating rapid inactivation as typical batch studies involving silver nanoparticles take on the order of hours to achieve such inactivation. These results are promising for the development of nanomaterials capable of utilizing microwave radiation; however, efficiency will need to be increased in order to treat larger volumes of water. Incorporating various nanomaterials with several stress-inducing mechanisms has the potential to enable irradiation-based disinfection with the globally-diffused microwave oven for treatment at the household level.

Table of Contents

List of Tables

List of Figures

1. Introduction

1.1 BACKGROUND

The 2030 Agenda for Sustainable Development recognized access to water, sanitation, and hygiene as human rights and the world leaders agreed to target universal and equitable access to safe and affordable drinking water for all.[1] The World Health Organization (WHO) estimated that as recently as 2015, over 663 million people lacked access to an improved drinking water source.[1] Providing safe drinking water is a multifaceted problem that goes beyond a treatment device and deserves a holistic approach with respect to sanitation, handling, education, and customs of the target community. Point-of-use (POU) treatment at the household or community level alleviates concerns regarding recontamination, however the ease of integration into a community is imperative for implementation of a technology. Socially-embedded technologies based on familiar components are more likely to receive prolonged use from the residents.[2–5]

Common knowledge indicates that access to clean water is limited in Sub-Saharan Africa and Asia. However, nearly 10% of those that do not have access to safe water live in developed regions, including North- and Meso-America. For example, in the southern Mexican states of Oaxaca and Chiapas, 40% of residents are deprived of a municipal water source.[6] The children of Oaxaca have especially suffered from rampant parasitism and from a high rate of infant mortality.[7] Rowles et al. (2018) surveyed residents in multiple rural Oaxacan communities and discovered a discrepancy between perceived and actual water quality. The majority of the residents believed that their water was safe to drink, despite the varying levels of fecal coliforms that were detected.[8] The study also showed that the residents of these communities relied heavily on purchased bottled water

for drinking, which accounted for at least 4% of their monthly income. A similar study is currently underway at the *colonias*, which are communities with self-built houses along the Texas-Mexico border.[9] Residents of the *colonias* have also suffered from waterborne diseases (e.g., cholera outbreaks) and have resorted to spending an average of 7% of their monthly income on bottled water.[10,11] Purchasing bottled water adds unnecessary economic stress on already economically challenged areas. Affordable and appropriate treatment technologies need to be developed for such low-income communities.

Irradiation-based disinfection technologies have increasingly become preferred over chemical disinfection methods, such as chlorination, to generally avoid the formation of carcinogenic disinfection by-products (DBPs).[12,13] Ultraviolet radiation is a common non-chemical disinfection technique; however, it may not be available nor affordable in low-income areas. As an alternate radiation source, microwaves (MWs) could be attractive. MW ovens are a globally diffused technology and present an accessible source of irradiation for household water treatment. For example, of the *colonias* residents surveyed, 95% of homes reported owning a MW. The unintended benefit of MWs to provide safe drinking water holds immense potential for a large global population. Though MW radiation can be widely accessible, the low energy potency of this electromagnetic radiation does not make it energetically favorable for disinfection. However, engineered nanomaterials can absorb MW radiation, facilitate interfacial energy transfer, and thus possibly enable disinfection. Nanomaterials have been used extensively for antimicrobial purposes through several biological stresses: oxidative[14–16], ion-mediated[17–19], particulate[20], and heat shock. A successful disinfection strategy could deliver an array of stress-inducing mechanisms for optimal inactivation.

1.2 OBJECTIVES

This study resides at the interface of nanotechnology and water disinfection, using MW energy to develop a socially-embedded POU strategy. The objective of this study is to demonstrate a synergistic effect between MW radiation and silver nanoparticles (AgNPs) where the antimicrobial properties of AgNPs are significantly enhanced. It is hypothesized that the heating from MW radiation will induce greater ion dissolution and interfacial heating in AgNPs, thus enhancing inactivation of bacteria. Carbon nanotubes (CNTs) have a high heat conductance and MW absorptivity.[51,52] Attaching AgNPs to the surface of CNTs can potentially increase the efficiency of inactivation mechanisms as CNTs concentrate and localize the radiation.

2. Literature Review

2.1 NANO-ENABLED DISINFECTION

Silver has been used as a broad spectrum antimicrobial agent in various medical and consumer product applications. Recently, silver nanoparticles (AgNPs) have received particular attention for drinking water disinfection and have been incorporated into a number of porous supports for POU treatment including cellulose paper[21], ceramics[22,23], carbon[24–26], polyurethane foam[27], and polystyrene beads[28], among others. The toxicity of silver ions (Ag^+) to bacteria has been well documented and might be related to outer membrane disruption and reactions with thiol-containing proteins, DNA, and respiration enzymes.[29–31] The release of free silver ions ($Ag^+_{(aq)}$) via oxidative dissolution is thought to be a primary component of AgNP toxicity.[32,33] The antimicrobial properties of particulate silver are enhanced at the nano-scale where AgNPs are in contact with cells and dissolved ions are localized at the outer membrane.[31,34] Additional mechanisms of inactivation for the particulate form of silver include physical disruption of the cell membrane[35] and photogeneration of reactive oxygen species (ROS)[36,37], a class of radical and non-radical forms of high energy chemical species, e.g., hydrogen peroxide (H_2O_2) and hydroxyl radicals ($OH\bullet$). Interaction of ROS at the cell surfaces can induce membrane leakage by lipid peroxidation or protein oxidation.[38] Smaller nanoparticles (<10 nm) can penetrate cells and inactivate bacteria via DNA damage once inside the cell.[38,20] Oxidative stress can also be caused by AgNP via intracellular ROS accumulation upon disruption of the cell membrane and electron transport chain.[39]

2.2 MICROWAVE UTILIZATION

Silver ion release is an oxidative process driven by oxidative agents such as H_2O_2 or dissolved oxygen. The basic stoichiometric reaction is as follows:

$$2Ag_{(s)} + \frac{1}{2}O_{2(aq)} + 2H^{+}{}_{(aq)} \rightarrow 2Ag^{+}{}_{(aq)} + H_2O_{(l)}$$

This oxidative dissolution is clearly a function of pH with increased dissolution at lower pH values. Dissolution rate also is highly dependent on particle size, surface functionalization, particle crystallinity, and temperature.[17] Liu and Hurt (2010) showed an approximate 2-fold increase from a temperature increase of 20 °C to 37 °C at short incubation times.[40] Kittler et al. (2010) also analyzed dissolution rates as a function of temperature (25 °C and 37 °C), albeit at significantly higher concentrations and time spans as compared to the values used in the current study.[17] The increase in dissolution with increasing temperature was also clearly demonstrated but interestingly, the concentration of ions in solution was independent of the amount of solid AgNP present. This indicated dissolution as a temperature-dependent, intrinsic property of nanoparticles that is not fully understood.

In heat-transfer applications, the suspension of metal nanoparticles in base fluids has been utilized to enhance thermal conductivity of otherwise low conducting fluids such as water or oil.[41,42] Silver has the highest thermal conductivity (406 W/m K) among metals, and suspending AgNPs has been shown to increase thermal conductivity as size decreases and/or concentration increases.[43–45] Thermal treatment of bacteria is a commonly used method in food preservation and has been shown to damage cell structures and DNA, possibly via oxidative stress.[46–48] Transcriptomic analysis of *Escherichia coli* reveals a heat shock response consisting of a rapid increase in production of the alternative σ factor RpoH (σ^{32}) at temperatures above 42 °C.[49,50] The addition of AgNP to bacterial cultures may increase the thermal conductivity of the solution, thus decreasing the energy input required to elicit a heat shock response.

3. Materials and Methods

3.1 NANOPARTICLE SYNTHESIS

3.1.1 Citrate-Capped Silver Nanoparticles

Citrate was used as the capping agent for AgNPs and these particles were synthesized according to a well-established protocol that uses sodium borohydride as the reducing agent.[53,54] Two reagents, i.e., 1.69 mL of 58.8 mM $AgNO_3$ and 2.92 mL of 34 mM sodium citrate, were added to 400 mL boiling ultrapure water with vigorous stirring. Subsequently, 2 mL of 100 mM $NaBH_4$ was added drop-wise in 100 μL increments and the solution continued to boil for 30 min with continuous stirring. Once cooled to room temperature, the aqueous suspension of AgNPs was purified in a nitrogen-pressurized stirred cell with a 3-kDa relative molecular weight cut-off regenerated cellulose ultrafiltration disc (Millipore, Billerica, MA) and was later stored at 4 °C.

3.1.2 Functionalized CNTs

Pristine multi-walled carbon nanotubes (MWNTs; outer diameter of 8–15 nm) were purchased from Cheap Tubes Inc. (Brattleboro, VT). MWNTs need to be functionalized with carboxylic groups on the surface to debundle and increase their dispersion in water. The functionalization process began with ultrasonication of 1.0 g of MWNTs combined with 150 mL of both concentrated nitric (70%) and sulfuric acid (96.5%). Once sonicated, the suspension was transferred to a 3-neck flask in a reflux apparatus consisting of a heat mantle and recirculating cooler to trap condensation and minimize losses. The CNTs were oxidized by the mixture of nitric and sulfuric acids under reflux for 3 hours at 80 °C to induce carboxylic groups on the surface and remove impurities. The contents were subsequently washed with ultrapure (Milli-Q, EMD

Millipore, Darmstadt, Germany) deionized water (DI) and vacuum-filtered using porous polytetrafluoroethylene (PTFE) membrane filters (0.2 μm, EMD Millipore, Darmstadt, Germany). Finally, the filters were dried in a desiccator for 48 hours and the resulting mass was scraped off and ground to a fine powder with a mortar and pestle to a fine powder.

3.1.3 Silver-Decorated CNTs

Silver-decorated CNT synthesis was performed with $AgNO_3$ as the Ag salt, functionalized MWNTs (f-MWNTs), and dimethylformamide (DMF) as the reducing agent following a published protocol.[55] First, 100 mg of f-MWNTs were added to 52 mL of DMF and ultrasonicated for 30 min and then placed in a water bath at 60 °C with vigorous stirring. Then, 12 mL of 0.1 M $AgNO_3$ solution was added drop-wise via a peristaltic pump. The reaction was allowed to proceed at 60 °C for one hour upon complete addition of $AgNO_3$. The suspension was then stored overnight at room temperature with continuous stirring to prevent settling of particles. Finally, the particles were washed with acetone, ethanol, and ultrapure DI water sequentially and then vacuum-filtered using porous polytetrafluoroethylene (PTFE) membrane filters (0.2 μm)

3.2 CHARACTERIZATION

Nanoparticle size analysis was performed using by high-resolution transmission electron microscopy (TEM; JEOL 2010F HRTEM) at various magnifications and at an accelerating voltage of 200 kV. Image processing and size analysis were subsequently performed using ImageJ software. Size of the colloidal AgNP suspension was determined with dynamic light scattering (DLS). An ALV/CGS-3 compact goniometer system (ALV-Laser Vertriebsgesellschaft m-b.H., Langen/Hessen, Germany) equipped with a 22

mW He/Ne 632 nm laser and a high-QE APD detector with photomultipliers of 1:25 sensitivity was used. All measurements were made at a scattering angle of 90° and the autocorrelation function was accumulated over 15-s time stamps.

3.3 BACTERIAL GROWTH

E. coli (ATCC 15597) was used as the model microorganism for inactivation experiments. Freezer stocks were stored at -80 °C for prolonged durations. Luria Bertani (LB) broth and agar plates were used for growth of bacteria. Freezer stock was streak-plated onto LB agar and incubated at 37 °C for 16-24 hours. An individual colony was retrieved with a sterile inoculating loop, placed in 25 mL of LB broth, and inoculated overnight on a shaker at 200 rpm and 37 °C. To ensure viability, 6 mL of sterilized 100% glycerol was added to the overnight culture and vortexed. The solution was divided into 1-mL aliquots and stored in sterile cryogenic vials at -80 °C. This process of developing frozen working cultures enhances the repeatability of experiments as all cultures were grown under the same conditions.

At the beginning of a new experiment, one aliquot of the frozen working culture was added to 25 mL of LB broth in a 250-mL Erlenmeyer flask, inoculated at 37 °C, and shaken for 12-16 hours. The following day, 15 mL of LB medium was inoculated with 100 μL of the overnight culture and grown at 37 °C until mid-exponential phase (~2.5 hours). Growth of the bacteria was determined by the optical density (OD) of the culture at a wavelength of 600 nm using a Synergy-HT microplate reader (Biotek, Winooski, VT).

3.3.1 Exposure Solutions

To prevent cell growth and maintain pH during experiments, cells were washed and

suspended in a buffer solution that resembled alkalinity and ionic strength of natural water. This synthetic water buffer was designed to limit osmotic shock of the bacteria as well as to minimize aggregation of the nanoparticles.[56,57] Specific considerations for AgNPs mainly involved omitting chloride because high chloride concentrations have been known to cause silver chloride formation as well as aggregation.[58,59] The buffer has an alkalinity of 200 mg/L as $CaCO_3$ and an ionic strength of 10 mM. This solution was prepared by dissolving 328 mg of $NaHCO_3$ and 513 mg of $Mg(NO_3)_2$-$6H_2O$ in 1 L of ultrapure water and adjusting pH to 8.3. This solution was autoclaved prior to use.

3.4 TOLERANCE EXPERIMENTS

Tolerance experiments were performed with a MW reactor system consisting of a MW power generator (GMP150, Opthos Instruments Inc., Rockville, MD) and a coaxial cable that transmits radiation to a waveguide and copper reactor. The operating frequency of the generator is 2.45 GHz ± 25 MHz and input power varies from 1-150 W.[60] A schematic and images of the reactor are included in **Figure A-1** of the Appendix.

Once the acclimated working culture of *E. coli* reached mid-exponential phase growth (OD at 600 nm of 0.25-0.30), the solution was centrifuged (5810R, Eppendorf AG, Hamburg, Germany) at 5,000×g for 15 min, and the supernatant was removed. The remaining cell residue was washed and re-suspended in the buffer solution. The solution was centrifuged and washed two additional times to ensure complete removal of growth medium. Meanwhile, a stock of 10 mg/L AgNPs in DI was bath-sonicated for approximately 10 min. Samples were prepared by adding 100 μL of the AgNP stock to 900 μL of the bacteria suspension for a final AgNP concentration of 1 mg/L. In no-AgNP control samples, 100 μL of buffer solution was added in lieu of the AgNP stock. The samples were then irradiated at 2,450 MHz and 70 W for various exposure times as these

MW control parameters typically represent a sufficient baseline for inactivation assays.[60] Following irradiation, reactions were allowed to proceed for 5 min and then 10μL of neutralizer solution (0.1 N sodium thiosulfate) was added to the irradiated mixture. Thiosulfate complexes with silver ions in solution and thus inhibits microbial interaction.[61–63] The neutralizer solution was prepared by dissolving anhydrous sodium thiosulfate in DI water followed by autoclaving. The irradiated samples were then immediately serially diluted up to 6 orders of magnitude using the buffer solution. Finally, 10 μL of each dilution was spot-plated onto LB agar plates in triplicate, incubated for 12-16 hours at 37 °C, and colony forming units (CFU) counted. A target of 10-30 CFUs/spot was used to select the dilution to count.

3.5 SILVER ION DISSOLUTION

To quantify the concentration of AgNP in the synthesized stock solutions, 10 mL samples of AgNP diluted to various concentrations with ultrapure water were prepared and digested in 0.77 mL of concentrated nitric acid (65-70%), overnight. Calibration curves were based on serial dilutions of a silver nitrate standard (SpexCertiPrep, Metuchen, NJ) in ultrapure water using a Varian 710 (Agilent, Santa Clara, CA) inductively coupled plasma−optical emission spectrometer (ICP-OES) with an approximate limit of detection of 5 μg/L.

Aqueous free silver released before and after MW irradiation was quantified by sampling AgNP suspensions under the same conditions as the tolerance experiment. These solutions were then diluted to 5 mL with ultrapure water and centrifuged in a Microsep™ Advance Centrifugal Filter with a 3 kDa MWCO (Pall Laboratory, Port Washington, NY) for 25 min at 5,000 × g. The permeate was digested in 0.385 mL of concentrated nitric acid overnight and analyzed with ICP-OES.

3.6 MICROWAVE HEATING

The bulk change in temperature of the samples was measured by a k-type beaded wire stainless steel thermocouple (SC-GG-K-30-36, Omega, Stamford, CT) before and after MW irradiation. Each sample contained 1 mL of solution and was placed in a quartz tubes. Quartz was chosen for all samples because of the minimal MW radiation absorbed as indicated by the low dielectric loss factor ($\varepsilon_r^{"} = 0.0001$). The thermocouple was connected to a digital thermometer (CL3512A, Omega, Stamford, CT), with a temperature range of -220 to 1372 °C. The thermocouple probe was completely submerged and the maximum temperature measured was recorded as the system quickly decreased in temperature once removed from the MW reactor.

4. Results

4.1 CHARACTERIZATION

TEM images of the colloidal AgNP suspension presented in **Figure 4-1** display the spherical nature of the particles. The lattice fringes are visible in the high-resolution image of **Figure 4-1(b)** and correspond to a d-spacing of 0.24 nm, which is consistent with the expected (1,1,1) crystal plane of AgNPs.[64] The average diameter of the AgNPs is 13.6 ± 2.5 nm, and the size distribution is shown in **Figure 4-2**.

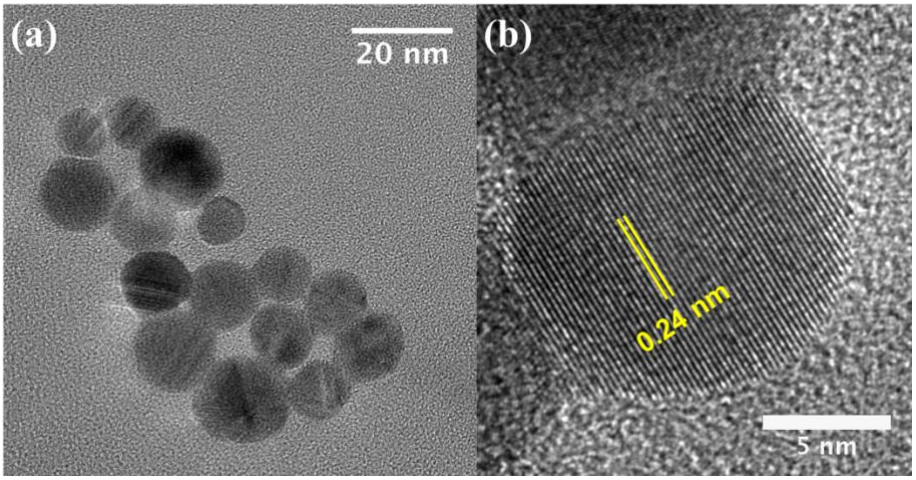

Figure 4-1: Representative HRTEM micrographs of silver nanoparticles; (a) shows spherical nature and (b) shows the lattice fringes with a d-spacing of 0.24.

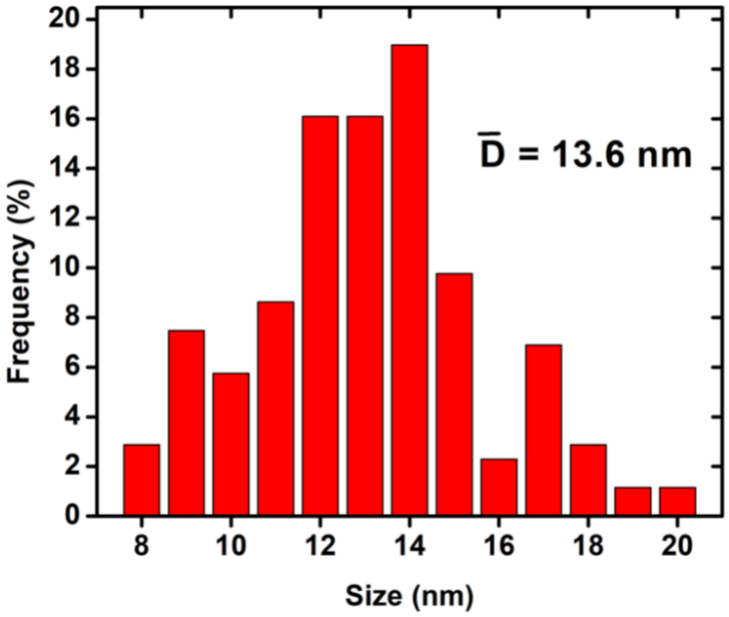

Figure 4-2: Size distribution of citrate-capped AgNP from TEM analysis. Average diameter measured was 13.6 nm with a standard deviation of 2.5 nm.

Aggregation kinetics in DI and the buffer solution (used for tolerance experiments) was analyzed with DLS and is reported in **Figure 4-3**. AgNPs remained stable in DI over the time span analyzed with an average hydrodynamic diameter of 54.4 ± 2.6 nm. The citrate capping agent is a relatively small organic molecule and not expected to influence the hydrodynamic radius; therefore, the 4-fold increase in diameter is most likely attributed to clustering of the nanoparticles. In the synthetic water buffer solution, AgNPs aggregate rapidly from the moment of addition. This is not a desired result as aggregation limits surface processes such as ion dissolution; however, AgNPs are not suspended in the buffer solution beyond 10 min so the impact may be minimized. If aggregation does present an issue in future assays, this can be mitigated by replacing the divalent Mg^{2+} with a monovalent cation such as Na^{+}.[65]

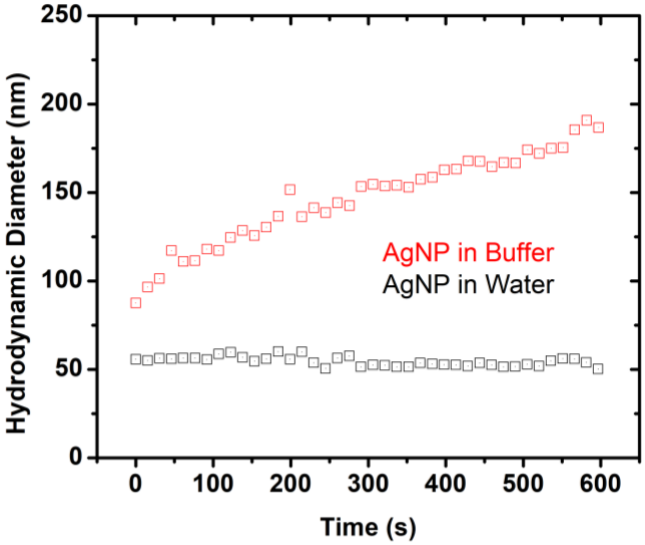

Figure 4-3: Particle size history of AgNPs in DI (black) and in synthetic buffer solution (red) as measured with DLS.

4.2 SILVER TOLERANCE ASSAYS

Inactivation of *E. coli* was analyzed at varying AgNP concentrations (0.5 and 1 mg/L) as well as with different MW irradiation times (0, 60, and 90 s). MW control parameters were set at a frequency of 2,450 MHz and input power of 70 W for all assays. Inactivation results are displayed in **Figure 4-4**, which show a clear trend of increased inactivation with the increase in AgNP concentration and MW irradiation time. As noted in the figure, the cells exposed to 1 mg/L AgNP and 90 s of MW treatment are inactivated beyond the detection limit; thus the $\log_{10}$ reduction is at least 4.67 but might be higher. Increasing the initial population density of *E. coli* will be needed to elucidate a more accurate level of inactivation. Examples of incubated plates following an experiment is presented in **Figure 4-5**.

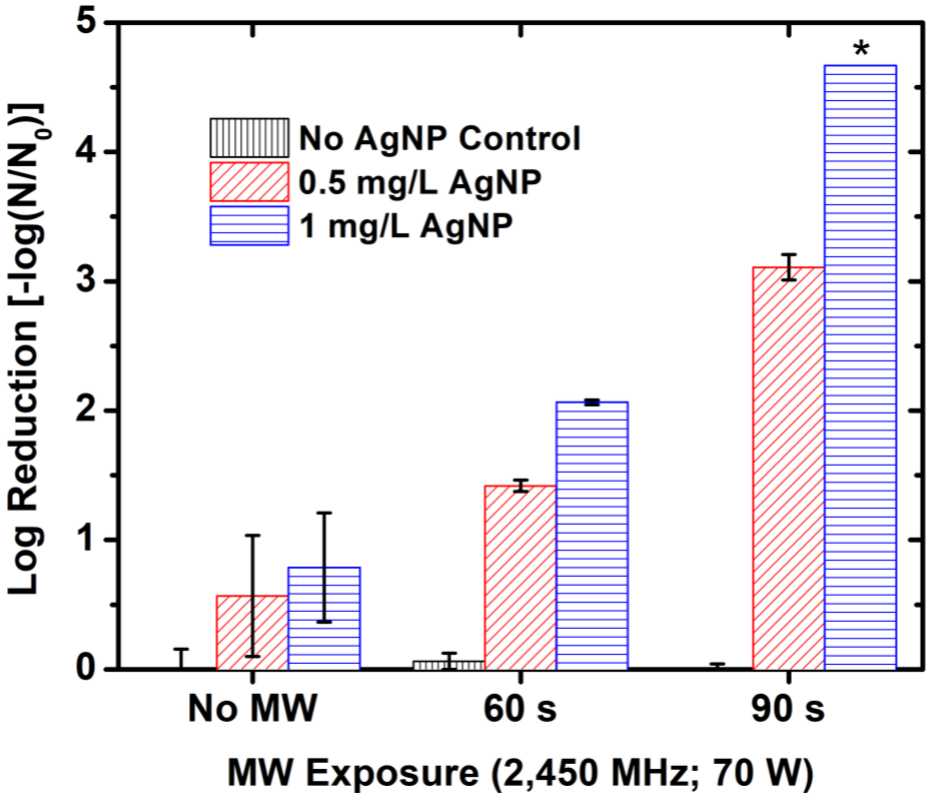

Figure 4-4: Log reduction of *E. coli* exposed to AgNP and irradiated with MW for various times. Initial concentration of *E. coli* was maintained between $10^{6.6}$ and $10^{6.7}$ CFU/mL. Error bars represent one standard deviation taken from triplicate measurements. **indicates removal beyond detection limit*

Of particular significance to this study is the observed synergistic impact from nanoparticle and MW irradiation. In control experiments with no AgNPs, exposure to MW had a negligible effect on inactivation. Adding 60 s of MW irradiation to the 1 mg/L AgNP samples increased inactivation potency from 0.8 to 2.1 $\log_{10}$ removal. Further, this rapid decrease in viable counts is promising. Silver antimicrobial studies are highly dependent on water composition and experimental parameters; however, comparing the current results to existing literature highlights the implication of these findings. Patil et al. (2013) surveyed a variety of POU disinfectants in batch *E. coli* inactivation studies

(initial cell concentration of 10^6 CFU/mL) and found that a contact time of 2 h with 1 mg/L of citrate-capped AgNPs was required for 1 mg/L of citrate-capped AgNP to reach 5 $\log_{10}$ removal.[62] In the case of silver ions, less than 2 $\log_{10}$ of removal was achieved after a 2-h contact time. Gangadharan et al. (2010) performed an immersion test using 200 mg of AgNP-coated copolymer beads and an initial *E. coli* concentration of $7x10^6$ CFU/mL.[66] After 4 h of contact time 6 $\log_{10}$ of removal was observed. Lv et al. (2009) tested silver-decorated porous ceramic tiles and in a batch test observed 4-5 $\log_{10}$ removal after 24 h.[23] These results are summarized in **Table 4-1**. Overall, the results from this study compare favorably as similar reductions in viable counts were achieved, but at a fraction of the exposure time.

Table 4-1: Summary of AgNP antimicrobial efficacy in various applications

Reference	**Silver Conc.**	**Silver Type**	***E. coli* Conc.**	**Exposure time**	**Inactivation**
Patil et al (2013)[62]	1 mg/L	Citrate-capped AgNP	10^6 CFU/mL	2 h	5 log
Gangadharan et al. (2010)[66]	200 mg	Copolymer microspheres	$7x10^6$ CFU/mL	4 h	6 log
Lv et al. (2009)[23]	0.044 g/cm^2	Porous ceramic tiles	10^4–10^5 CFU/mL	24 h	4-5 log

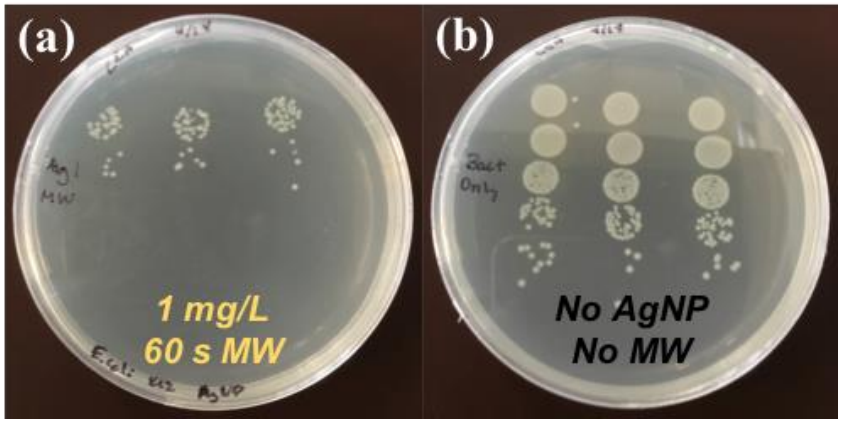

Figure 4-5: Example plate counts from (a) inactivation of *E. coli* exposed to AgNPs and MW, (b) control – *E. coli* with no AgNPs and no MW. MW was operated at a frequency of 2,450 MHz and input power of 70 W.

4.3 SILVER DISSOLUTION

To evaluate the mechanisms of action, it is necessary to test the hypothesis of silver dissolution and temperature increase with MW irradiation. This theory was analyzed by filtering a 1 mg/L AgNP suspension and analyzing it with ICP-OES. Preliminary results from 0, 60, and 90 s of MW irradiation are presented in **Figure 4-6(a)**. Temperature change from the same MW treatment is displayed in **Figure 4-6(b)**.

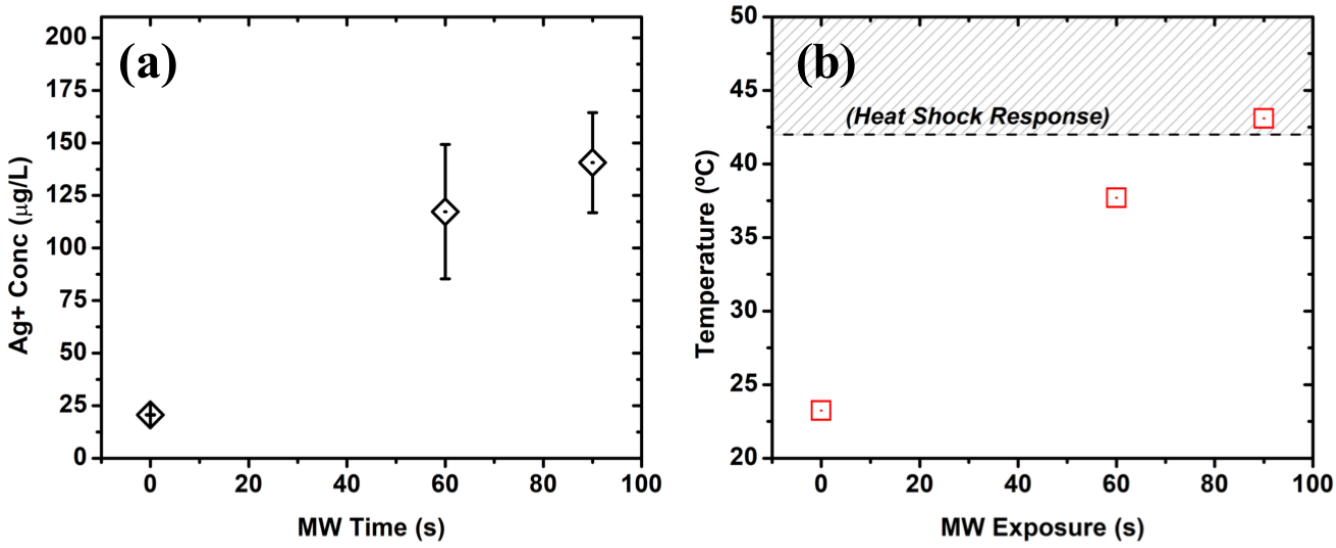

Figure 4-6: (a) Silver ion dissolution from 1 mL of 1 mg/L AgNP samples diluted with DI water before and after MW treatment; (b) Temperature of 1 mg/L AgNP in DI sample before and after MW treatment. Dashed line refers to temperature where a heat shock response in *E. coli* is known to be induced.[49] MW in both instances was operated at a frequency of 2,450 MHz and input power of 70 W.

Dissolution increased with the increase in irradiation time; however, the results are accompanied by a significant margin of error. The source of this error is believed to be in the dilution required for assay and analysis. For consistency with the tolerance experiments, 1 mL of sample was analyzed. ICP-OES requires a minimum of 5 mL for analysis and therefore, the samples had to be diluted. The concentrations measured were thus minimal and within the margin of error of the instrument. Additional studies will seek the use of a graphite furnace that requires a much lower sample volume, and is anticipated to produce more accurate results for low concentrations.[21,40]

Temperature of the AgNP and DI sample in **Figure 4-6(b)** increased 14.5 °C and 19.9 °C following MW exposure of 60 s and 90 s, respectively. A dashed line is shown in **Figure 4-6(b)** at 42 °C where heat shock response has been observed previously for *E.*

coli.[49] The sample irradiated for 90 s exceeded this threshold. Samples of DI, buffer solution, and AgNPs in the buffer solution yielded similar results. This was unexpected considering the heat conductivity of silver; however, these results simply reflect the bulk heating of the samples. Interfacial heating is required to be determined for better assessment of heat transfer from AgNPs.

4.4 SILVER-DECORATED CNTS

To improve bacterial inactivation from MW irradiation, the use of MWNTs (with high MW absorbability) is preferred for the preparation of nanohybrids with AgNPs. Silver-MWNT nanohybrids have been prepared as shown in the TEM micrographs presented in **Figure 4-7.** The micrographs reveal spherical silver nanoparticles formed on the MWNTs at a size range of 10-15 nm in diameter. However, attachment of all such particles is not completely confirmed. As seen in **Figure 4-7(c)**, several particles appear to be isolated from the f-MWNTs and might be co-associating with the MWNTs or suspended independently. The silver particles in **Figure 4-7(b)** appear to be possibly hybridized, and thus gives some promise to these preliminary results for the hybrid preparation**.**

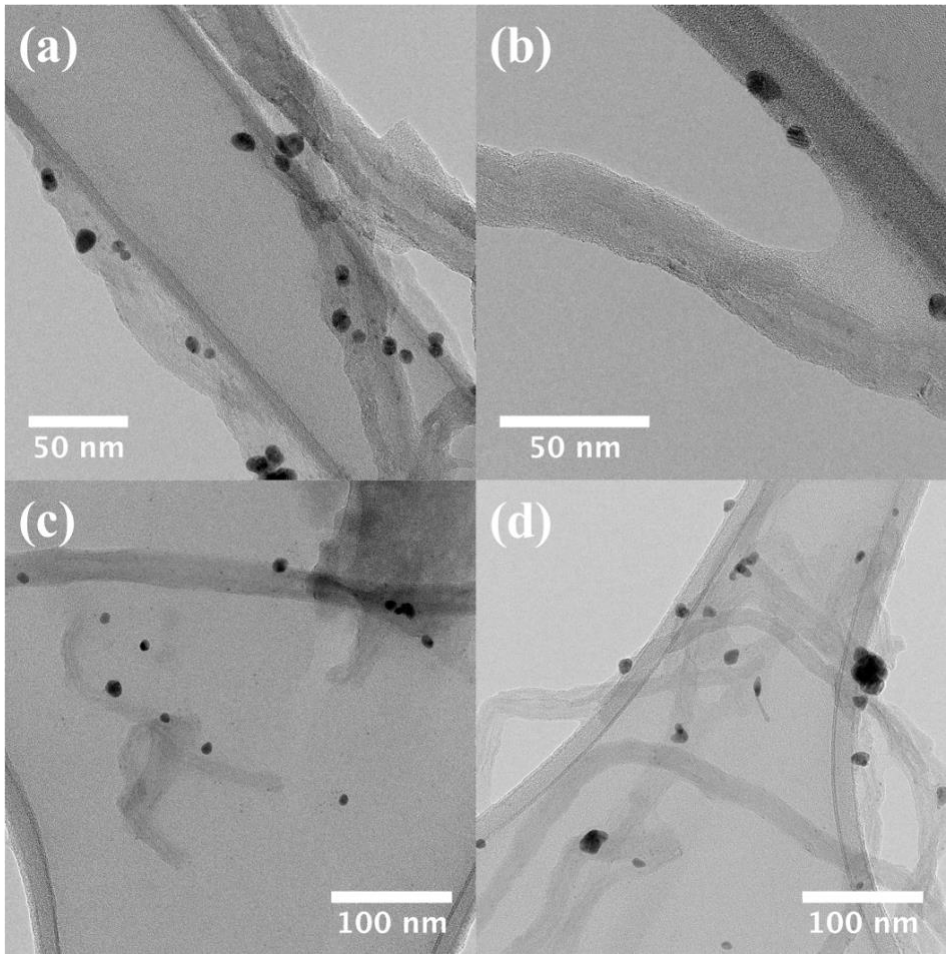

Figure 4-7: Representative TEM micrographs of Ag-MWNT hybrids

5. Conclusions

5.1 Discussion of Findings

This study resides at the interface of nanotechnology and water disinfection, using the global diffusivity of MW technology and the exceptional properties of nanomaterials to develop an effective alternative for disinfection. A clear synergistic effect between MW irradiation and silver exposure was elucidated with increased inactivation at increased exposure times and silver concentrations. Plazas-Tuttle et al. (2018) also demonstrated a synergistic effect between a novel erbium-CNT hybrid material and MW radiation.[67] Lanthanide series metals such as erbium (Er) are capable of spectral upconversion, a complex process characterized by the successive absorption of two or more pump photons via intermediate long-lived energy states followed by the emission of the output radiation at a shorter wavelength than the pump one.[68] The Er-CNT hybrid was capable of upconverting MW radiation to produce ROS and inactivate over one $\log_{10}$ reduction of *Pseudomonas aeruginosa* with 20 s of exposure in a conventional microwave oven (110 W). However, the antimicrobial potency plateued below 2 $\log_{10}$ reduction, possibly due to aggregation. A hybrid material comprised of both AgNP and Er would utilize several mechanisms of inactivation. Increasing the antimicrobial potency and efficiency is critical for scaling up the volume treated because of the additional energy input required to heat larger volumes of water. Preliminary hybridization procedures involving AgNP and f-MWNT were promising but progress still needs to be made on the attachment mechanism before use in tolerance assays can be examined.

5.2 Future Work

The World Health Organization (WHO) established microbiological performance targets for POU technologies with $\log_{10}$ inactivation requirements for bacteria ($\geq$ 4),

viruses ($\geq$ 5), and protozoa ($\geq$ 4) under a variety of water quality characteristics.[63] This study focused solely on one bacterial species (*E. coli*) in consistent exposure solutions. The experimental matrix will need to be expanded to incorporate various conditions this strategy would encounter in real applications. Growing microorganisms in a chemostat reactor would reduce the stress from centrifuging and washing and would allow for improved repeatability among experiments. Before expanding the experimental matrix, however, further work is required on the mechanistic study of AgNPs under MW irradiation. This work may include an ROS probe, more accurate dissolution studies, and a transcriptomic analysis to determine gene regulation and how the bacteria respond to certain treatments. There is potential for more efficient inactivation by customizing the capping agent with desired properties such as high heat conductance or enhancing the attachment of AgNP to bacteria with electrostatic attraction or chain length. Ultimately, hybrid materials incorporating a suite of mechanisms of inactivation need to be synthesized and the device engineering phase will emphasize immobilization of the materials on a ceramic tablet or flow-through membrane.

Appendix

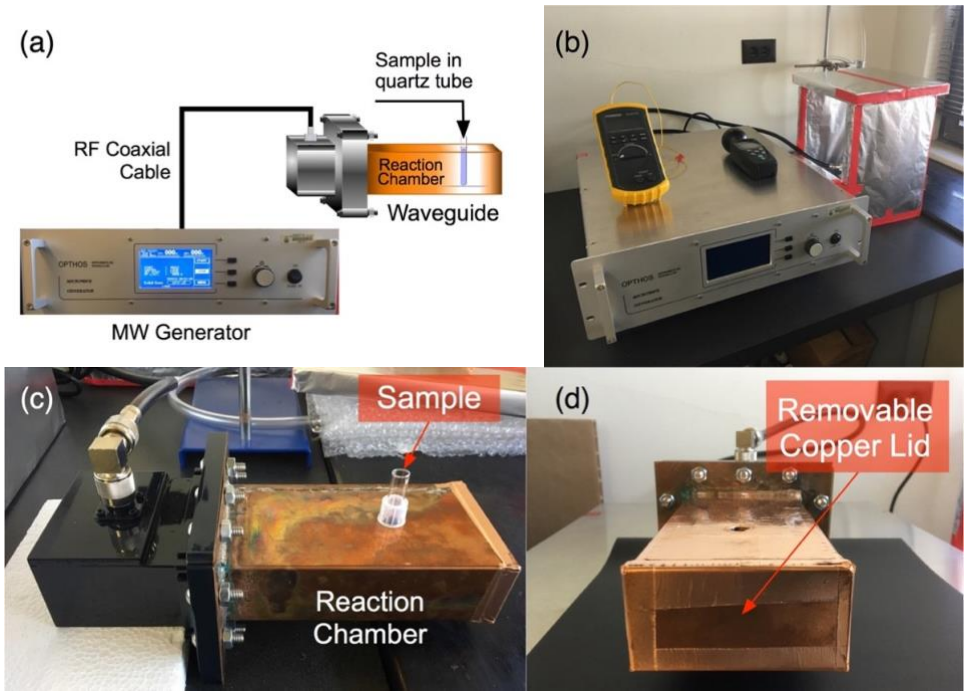

Figure A-1: (a) Schematic representation of the MW setup, (b) MW power generator, (c) waveguide and copper reaction chamber, (d) closed end of the copper reaction chamber.[60]

References

1. WHO/UNICEF. *Progress on Drinking Water, Sanitation and Hygiene: 2017 Update and SDG Baselines*. (2017). doi:10.1111 / tmi.12329
2. Osterwalder, L., Johnson, C. A., Yang, H. & Johnston, R. B. Multi-criteria assessment of community-based fluoride-removal technologies for rural Ethiopia. *Sci. Total Environ.* **488–489,** 532–538 (2014).
3. Rosa, G., Kelly, P. & Clasen, T. Consistency of Use and Effectiveness of Household Water Treatment Practices among Urban and Rural Populations Claiming to Treat Their Drinking Water at Home: A Case Study in Zambia. **94,** 445–455 (2016).
4. Kallman, E. N., Oyanedel-craver, V. A., Asce, A. M., Smith, J. A. & Asce, M. Ceramic Filters Impregnated with Silver Nanoparticles for Point-of-Use Water Treatment in Rural Guatemala. *J. Environ. Eng.* **137,** 407–415 (2011).
5. Levine, D., Ave, O. R. & Francisco, S. End-User Preferences for and Performance of Competing POU Water Treatment Technologies among the Rural Poor of Kenya. **44,** 4426–4432 (2010).
6. Oswald Spring, U. Aquatic systems and water security in the Metropolitan Valley of Mexico City. *Curr. Opin. Environ. Sustain.* **3,** 497–505 (2011).
7. Quihui, L. *et al.* Role of the employment status and education of mothers in the prevalence of intestinal parasitic infections in Mexican rural schoolchildren. *BMC Public Health* **6,** 1–8 (2006).
8. Rowles III, L. S. *et al.* Perceived versus actual water quality: Community studies in rural Oaxaca,Mexico. *Sci. Total Environ.* **622–623,** 626–634 (2018).
9. Ward, P. M. *Colonias and public policy in Texas and Mexico: urbanization by stealth*. (University of Texas Press, 1999).
10. Jepson, W. & Brown, H. L. 'If no gasoline, no water': privatizing drinking water quality in South Texas colonias. *Environ. Plan. A Econ. Sp.* **46,** 1032–1048 (2014).
11. Rios, J. & Meyer, P. What Do Toilets Have to Do With It ? Health, the Environment, and the Working Poor in Rural South Texas Colonias. *Online J. Rural Res. Policy* **4,** 1–20 (2009).
12. Richardson, S. D. Disinfection by-products and other emerging contaminants in drinking water. *Trends Anal. Chem.* **22,** 666–684 (2003).
13. Zhou, H. & Smith, D. W. Advanced technologies in water and wastewater treatment. *Can. J. Civ. Eng.* **28 (S1),** 49–66 (2001).
14. Das, D., Chandra, B., Phukon, P. & Kumar, S. Synthesis and evaluation of antioxidant and antibacterial behavior of CuO nanoparticles. *Colloids Surfaces B Biointerfaces* **101,** 430–433 (2013).
15. Xia, T. *et al.* Comparison of the Abilities of Ambient and Manufactured Nanoparticles To Induce Cellular Toxicity According to an Oxidative Stress Paradigm. *Nano Lett.* **6,** 1794–1807 (2006).
16. Hirakawa, K., Hirano, T. & Medical, P. Singlet Oxygen Generation Photocatalyzed by TiO 2 Particles and Its Contribution to Biomolecule Damage.

35, 832–833 (2006).
17. Kittler, S., Greulich, C., Diendorf, J., Koller, M. & Epple, M. Toxicity of Silver Nanoparticles Increases during Storage Because of Slow Dissolution under Release of Silver Ions. *Chem. Mater.* **22,** 4548–4554 (2010).
18. Loza, K. *et al.* The dissolution and biological effects of silver nanoparticles in biological media. *J. Mater. Chem. B* **2,** (2014).
19. Wakshlak, R. B., Pedahzur, R. & Avnir, D. Antibacterial activity of silver-killed bacteria: the 'zombie' effect. *Sci. Rep.* **5,** 1–5 (2015).
20. Laha, D. *et al.* Shape-dependent bactericidal activity of copper oxide nanoparticle mediated by DNA and membrane damage. *Mater. Res. Bull.* **59,** 185–191 (2014).
21. Dankovich, T. A. Nanoparticles in paper for point-of-use water purification. *Environ. Sci. Nano* **1,** 367–378 (2014).
22. Oyanedel-Craver, V. A. & Smith, J. A. Sustainable Colloidal-Silver-Impregnated Ceramic Filter for Point-of-Use Water Treatment. *Environ. Sci. Technol.* **42,** 927–933 (2008).
23. Lv, Y. *et al.* Silver nanoparticle-decorated porous ceramic composite for water treatment. *J. Memb. Sci.* **331,** 50–56 (2009).
24. Seo, Y. *et al.* Antibacterial activity and cytotoxicity of multi-walled carbon nanotubes decorated with silver nanoparticles. *Int. J. Nanomedicine* **9,** 4621–4629 (2014).
25. Al, S., Gomez, V., Wright, C. J. & Hilal, N. Fabrication of antibacterial mixed matrix nanocomposite membranes using hybrid nanostructure of silver coated multi-walled carbon nanotubes. *Chem. Eng. J.* **326,** 721–736 (2017).
26. Mohan, R., Shanmugharaj, A. M. & Hun, R. S. An efficient growth of silver and copper nanoparticles on multiwalled carbon nanotube with enhanced antimicrobial activity. 119–126 (2010). doi:10.1002/jbm.b.31747
27. Jain, P. & Pradeep, T. Potential of Silver Nanoparticle-Coated Polyurethane Foam As an Antibacterial Water Filter. *Biotechnol. Bioeng.* **90,** 3–7 (2005).
28. Mthombeni, N. H., Mpenyana-monyatsi, L., Onyango, M. S. & Momba, M. N. B. Breakthrough analysis for water disinfection using silver nanoparticles coated resin beads in fixed-bed column. *J. Hazard. Mater.* **217–218,** 133–140 (2012).
29. Feng, Q. L. *et al.* A mechanistic study of the antibacterial effect of silver ions on Escherichia coli and Staphylococcus aureus. *J. Biomed. Mater. Res.* **4,** (2000).
30. Lok, C. *et al.* Proteomic Analysis of the Mode of Antibacterial Action of Silver Nanoparticles research articles. *J. Proteome Res.* **5,** 916–924 (2006).
31. McQuillan, J. S. & Shaw, A. M. Differential gene regulation in the Ag nanoparticle and Ag(+)-induced silver stress response in Escherichia coli: A full transcriptomic profile. *Nanotoxicology* **8,** 177–184 (2014).
32. Chambers, B. A. *et al.* Effects of chloride and ionic strength on physical morphology, dissolution, and bacterial toxicity of silver nanoparticles. *Environ. Sci. Technol.* **48,** 761–769 (2014).
33. Xiu, Z., Zhang, Q., Puppala, H. L., Colvin, V. L. & Alvarez, P. J. J. Negligible Particle-Specific Antibacterial Activity of Silver Nanoparticles. *Nano Lett.* **12,**

4271–4275 (2012).
34. Kurvet, I., Kahru, A., Bondarenko, O., Ivask, A. & Ka, A. Particle-Cell Contact Enhances Antibacterial Activity of Silver Nanoparticles. **8,** (2013).
35. Sondi, I. & Salopek-sondi, B. Silver nanoparticles as antimicrobial agent: a case study on E .coli as a model for Gram-negative bacteria. *J. Colloid Interface Sci.* **275,** 177–182 (2004).
36. Choi, O. & Hu, Z. Size Dependent and Reactive Oxygen Species Related Nanosilver Toxicity to Nitrifying Bacteria. *Environ. Sci. Technol.* **42,** 4583–4588 (2008).
37. Zhang, W., Li, Y., Niu, J. & Chen, Y. Photogeneration of Reactive Oxygen Species on Uncoated Silver, Gold, Nickel, and Silicon Nanoparticles and Their Antibacterial E ff ects. *Langmuir* **29,** 4647–4651 (2013).
38. Dutta, R. K., Nenavathu, B. P., Gangishetty, M. K. & Reddy, A. V. R. Studies on antibacterial activity of ZnO nanoparticles by ROS induced lipid peroxidation. *Colloids Surfaces B Biointerfaces* **94,** 143–150 (2012).
39. Cheng, X. *et al.* Revealing silver cytotoxicity using Au nanorods/Ag shell nanostructures: disrupting cell membrane and causing apoptosis through oxidative damage. *RSC Adv.* **3,** 2296–2305 (2013).
40. Liu, J. & Hurt, R. H. Ion Release Kinetics and Particle Persistence in Aqueous Nano-Silver Colloids. *Environ. Sci. Technol.* **44,** 2169–2175 (2010).
41. Palm, S. J., Roy, G. & Nguyen, C. T. Heat transfer enhancement with the use of nanofluids in radial flow cooling systems considering temperature-dependent properties. *Appl. Therm. Eng.* **26,** 2209–2218 (2006).
42. Paul, G., Sarkar, S., Pal, T., Das, P. K. & Manna, I. Concentration and size dependence of nano-silver dispersed water based nanofluids. *J. Colloid Interface Sci.* **371,** 20–27 (2012).
43. Godson, L., Raja, B., Lal, D. M. & Wongwises, S. Experimental Investigation on the Thermal Conductivity and Viscosity of Silver-Deionized Water Nanofluid. *Exp. Heat Transf.* **23,** (2010).
44. Young, H. D. *University Physics*. (1992).
45. Iyahraja, S. & Rajadurai, J. S. Study of thermal conductivity enhancement of aqueous suspensions containing silver nanoparticles. *AIP Adv.* **5,** 1–9 (2015).
46. Marcén, M., Ruiz, V., Serrano, M. J., Condón, S. & Mañas, P. Oxidative stress in E. coli cells upon exposure to heat treatments. *Int. J. Food Microbiol.* **241,** 198–205 (2017).
47. Bs, B. & I, R. I. S. The Effect of Catalase on Recovery of Heat-injured DNA-repair Mutants of Escherichia coli. (2018).
48. Nguyen, H. T. T., Corry, J. E. L. & Miles, C. A. Heat Resistance and Mechanism of Heat Inactivation in Thermophilic Campylobacters. **72,** 908–913 (2006).
49. Straus, D. B., Walter, W. A. & Gross, C. A. The heat shock response of E. coli is regulated by changes in the concentration of sigma-32. *Nature* **329,** 348–351 (1987).
50. Tomoyasu, T., Bukau, B. & Arsene, F. The heat shock response of Escherichia

coli. **55,** 3–9 (2000).
51. Che, J., Goddard III, W. A. & Cagın, T. Thermal conductivity of carbon nanotubes. *Nanotechnology* **11,** 65–69 (2000).
52. Chen, H. & Mcgaughey, A. J. H. Thermal conductivity of carbon nanotubes with defects. in *ASME/JSME 2011 8th Thermal Engineering Joint Conference* (2011).
53. Mikelonis, A. M. Adhesion of Silver Nanoparticle Amendments to Ceramic Water Filters. (University of Texas at Austin, 2015).
54. Gorham, J. M., Maccuspie, R. I., Klein, K. L., Fairbrother, D. H. & Holbrook, R. D. UV-induced photochemical transformations of citrate-capped silver nanoparticle suspensions. *J. Nanoparticle Res.* **14,** (2012).
55. Xin, F. & Li, L. Decoration of carbon nanotubes with silver nanoparticles for advanced CNT/polymer nanocomposites. *Compos. Part A* **42,** 961–967 (2011).
56. Afshinnia, K. & Baalousha, M. Effect of phosphate buffer on aggregation kinetics of citrate-coated silver nanoparticles induced by monovalent and divalent electrolytes. *Sci. Total Environ.* **582,** 268–276 (2017).
57. Chambers, B. A. *et al.* Effects of Chloride and Ionic Strength on Physical Morphology, Dissolution, and Bacterial Toxicity of Silver Nanoparticles. *Environ. Sci. Technol.* **48,** 761–769 (2014).
58. Li, X., Lenhart, J. J. & Walker, H. W. Dissolution-Accompanied Aggregation Kinetics of Silver Nanoparticles. *Langmuir* **26,** 16690–16698 (2010).
59. Tejamaya, M., Merrifield, R. C. & Lead, J. R. Stability of Citrate, PVP, and PEG Coated Silver Nanoparticles in Ecotoxicology Media. *Environ. Sci. Technol.* **46,** 7011–7017 (2012).
60. Plazas-Tuttle, J. Nano-Enabled Water Disinfection Technology Development that Harnesses the Power of Microwaves. (University of Texas at Austin, 2017).
61. He, D., Garg, S. & Waite, T. D. H2O2-mediated oxidation of zero-valent silver and resultant interactions among silver nanoparticles, silver ions, and reactive oxygen species. *Langmuir* **28,** 10266–10275 (2012).
62. Patil, R. A., Kausley, S. B., Balkunde, Pradeep, L. & Malhotra, C. P. Comparative study of disinfectants for use in low-cost gravity driven household water purifiers. *J. Water Health* **11,** 443–456 (2013).
63. World Health Organization. *WHO International Scheme to Evaluate Household Water Treatment Technologies*. (2014).
64. Sun, Y. & Xia, Y. Shape-Controlled Synthesis of Gold and Silver Nanoparticles. *Science (80-.).* **298,** 2176–2180 (2002).
65. Huynh, K. A. & Chen, K. L. Aggregation Kinetics of Citrate and Polyvinylpyrrolidone Coated Silver Nanoparticles in Monovalent and Divalent Electrolyte Solutions. *Environ. Sci. Technol.* **45,** 5564–5571 (2011).
66. Gangadharan, D. *et al.* Polymeric microspheres containing silver nanoparticles as a bactericidal agent for water disinfection. *Water Res.* **4,** 1–7 (2010).
67. Saleh, N. B., Plazas-tuttle, J., Das, D. & Sabaraya, I. V. Harnessing the power of microwaves for inactivating Pseudomonas aeruginosa with nanohybrids. *Environ. Sci. Nano* **5,** 72–82 (2018).

68. Li, X., Zhang, F. & Zhao, D. Highly efficient lanthanide upconverting nanomaterials : Progresses and challenges. *Nano Today* **8,** 643–676 (2013).